Aliphatic C–H bond scission processes in diphenylmethane and 2-benzyl- and 4-benzylpyridine. The heat of formation of the diphenylmethyl and α-phenylethyl radical in the gas phase

ARTICLE · OCTOBER 1984

CITATIONS
19

READS
5

3 AUTHORS, INCLUDING:

Michel J Rossi
Paul Scherrer Institut
259 PUBLICATIONS **6,487** CITATIONS

SEE PROFILE

fluoride affinity of BF_3, $D(BF_3-F^-)$, is then calculated to be 92.5 kcal/mol or 4 eV.

The electron affinity of BF_3 has been reported to be ≤ 0.0 eV[31] and as 2.65 eV,[32] but BF_3^- has not been observed. Since the addition of an electron to BF_3 would cause a change from planar to pyramidal geometry with an expected lengthening of the B-F bond length, it is easy to picture a vertical electron affinity of less than zero and a positive adiabatic electron affinity. This remains unresolved.

BF_4 has been described as unstable[30b] and as having a BF_3-F bond strength near zero.[10] However, the vertical electron affinity of BF_4 has been calculated to be 5.6 eV[33] with the estimate that the adiabatic EA differs by no more than 0.2-0.5 eV. If the vertical EA is accepted and combined with EA(F) = 3.4 eV[29b] and $D(BF_3-F^-)$ = 4.0 eV, then $D(BF_3-F)$ = 1.8 eV. If it is accepted that BF_4 is unstable, then by necessity $EA(BF_4) \leq 3.8$ eV.

Registry No. F^-, 16984-48-8; Cl^-, 16887-00-6; BF_3, 7637-07-2; BCl_3, 10294-34-5.

(31) Rothe, E. W.; Mathur, B. P.; Reck, G. P. *Inorg. Chem.* **1980**, *19*, 829.
(32) Page, F. M.; Goode, G. C. "Negative Ions and the Magnetron"; Wiley-Interscience: New York, 1969; p 139.
(33) Gutseve, G. L.; Boldyrev, A. I. *Chem. Phys.* **1981**, *56*, 277.

Aliphatic C-H Bond Scission Processes in Diphenylmethane and 2-Benzyl- and 4-Benzylpyridine. The Heat of Formation of the Diphenylmethyl and α-Phenylethyl Radical in the Gas Phase

Michel J. Rossi,* Donald F. McMillen, and David M. Golden

Department of Chemical Kinetics, SRI International, Menlo Park, California 94025
(Received: November 8, 1983)

Very low-pressure pyrolysis (VLPP) of the title compounds indicates both C-C and C-H bond rupture. Rate constants for all six processes are compatible with A factors of $10^{15.3}$ s^{-1} and activation energies of 81.4 kcal mol^{-1} for C-H rupture in diphenylmethane and 82.3 kcal mol^{-1} for all the other C-H and C-C bond-breaking processes. The derived heat of formation of diphenylmethyl radical is 69.0 kcal mol^{-1}. This is in excellent agreement with other studies and indicates that C-H bond rupture in phenylmethanes behaves analogously to C-C rupture. The "extra stabilization" in diphenylmethyl radical when compared with α-phenylethyl radical is ~4 kcal mol^{-1}.

Introduction

The need for thermodynamic data for free-radical intermediates is well recognized.[1] However, because the number of possible free-radical heats of formation that might be measured is too large to sensibly contemplate, prototypical species are usually determined and substituent effects are treated additively.

An important prototype is the benzyl radical ($PhCH_2$). Several studies involving benzyl radical he been performed in both gas and condensed phases.[2-4] A consensus value of $\Delta H_f°_{298}(PhCH_2,g)$ = 47.8 ± 1.5 kcal mol^{-1} has emerged.[1,5] Such a value leads to a bond dissociation energy (BDE) in toluene of 88 kcal mol^{-1} and thus a stabilization energy of ~10 kcal mol^{-1} compared with the C-H bond in ethane. Aromatic systems with more than one aromatic ring are, of course, common. In previous work we have addressed the question of stabilization in analogous polycyclic aryl radicals. Varying amounts of extra stabilization energy were found.[1] In this work we address the question of stability of diphenylmethyl radicals, the prototype itself as well as those derived from 2-benzyl and 4-benzylpyridine. The results, aside from their intrinsic interest, are relevant to understanding coal liquefaction processes, given the suspected prevalence of methylene linkages between aromatic coal subunits.

We have studied the decomposition of diphenylmethane and 2-benzyl- and 4-benzylpyridine using the VLPP technique.[6] At the reaction temperatures (1000-1300 K), there are two competitive decomposition pathways, C-H and C-C bond breaking:

$$Ph_2CH_2 \xrightarrow{a} PhCH_2 + Ph\cdot$$

$$\xrightarrow{b} Ph_2CH + H\cdot$$

Because the heats of formation of the radicals produced in path a are well established[1] and the A factor is easily estimated from analogous alkylbenzene decomposition reactions (see text), we may use the decomposition data to ascertain values for the activation energy of path b and thus the heat of formation of Ph_2CH.

The nature of the VLPP experiment requires that the A factor be known if the activation energy is to be determined. The A factor for path b can be estimated from that for toluene itself. However, there is a discrepancy between the A factor most workers report[3] for toluene decomposition ($A \sim 5 \times 10^{15}$ s^{-1}) and that reported in a shock-tube study,[7] which yielded extrapolated high-pressure parameters for $PhCH_3 \rightarrow CH_2 + H$ of $k/s^{-1} = 8 \times 10^{16} \exp(-90.8/RT)$ ($1100 < T/K < 1800$). In the present paper we resolve this discrepancy by comparing the values for the heat of formation of Ph_2CH, derived by using both the high and low A factors, with those derived from the VLPP studies of Robaugh and Stein.[8] They obtained Ph_2CH by pyrolyzing 1,1-diphenylethane, where all workers presently agree that a low A factor describes the $C-CH_3$ bond-breaking process.

Experimental Section

Very low-pressure pyrolysis (VLPP) as a method of obtaining absolute rate constants (uni- and bimolecular) has been described

(1) McMillen, D. F.; Golden, D. M. *Annu. Rev. Phys. Chem.* **1982**, *33*, 493-532.
(2) Robaugh, D. A.; Stein, S. E. *Int. J. Chem. Kinet.* **1981**, *13*, 445.
(3) Davis, H. A. *Int. J. Chem. Kinet.* **1983**, *15*, 469.
(4) Stein, S. E.; Robaugh, D. A.; Alfieri, A. D.; Miller, R. E. *J. Am. Chem. Soc.* **1982**, *104*, 6567-70.
(5) Rossi, M.; Golden, D. M. *J. Am. Chem. Soc.* **1979**, *101*, 1230.
(6) Golden, D. M.; Spokes, G. N.; Benson, S. W. *Angew. Chem., Int. Ed. Engl.* **1973**, *12*, 534.
(7) Astholz, D. C.; Durant, J.; Troe, J. In "Proceedings of the Eighteenth Symposium (International) on Combustion"; The Combustion Institute: Pittsburgh, PA, 1981; pp 885-92.
(8) (a) Robaugh, D. A. Ph.D. Thesis, West Virginia University, Morgantown, WV, 1983. (b) Stein, S. E. *ACS Symp. Ser.* **1981**, *No. 169*, 97.

0022-3654/84/2088-5031$01.50/0

in detail previously.[6] In short, the apparatus consists of a low-pressure Knudsen cell into which gases flow from a gas-handling system at higher pressure and from which they flow into a differentially pumped mass spectrometry chamber at lower pressure. The gas enters the Knudsen cell through 1-mm-i.d. inlet capillaries. An effusive molecular beam is formed at the exit aperture of the Knudsen cell. This beam impinges on the electron-impact ionizer of a mass spectrometer (Finnigan 400) after being chopped by an asynchronously driven motor at 90 Hz. The modulated portion of the total signal is recovered and rectified in a lock-in amplifier (PAR JB-5) and displayed on an X-Y recorder (Hewlett-Packard 7004B).

More specifically, the dual-aperture reactor used in the present study had a volume of 146 cm^3 and was characterized by two escape rate constants, $k_e^S = 0.175(T/M)^{1/2}$ s^{-1} and $k_e^L = 4.69(T/M)^{1/2}$ s^{-1}, where S is the small and L is the large aperture, T is the temperature in kelvin, and M is the molecular mass in amu. The reactor had a series of stopcocks that allowed the feed-gas to either enter the reactor through the 1-cm-long, 1-mm-diameter inlet capillary or bypass the reactor through a 1-cm-long, 1-mm-diameter capillary; the end of the bypass line was formed into a spout, which also formed an effusive molecular beam as the gases flowed into the high-vacuum chamber.

Because of the different geometries of the reactor exit aperture and the opening of the end ("spout") of the bypass line, the hydrodynamic properties of gas effusion as a function of temperature of the reactor were calibrated by monitoring a bypass-to-reactor ratio (B/R) of mass-spectral signal intensities as a function of temperature up the point where unimolecular decomposition sets in within the small-aperture reactor. Below this temperature, the bypass-to-reactor ratios provided a straight line when plotted as a function of temperature for both the small and large apertures. The unimolecular rate constants were calculated according to eq 1

$$k_{uni} = k_e[(B/R) - 1] \quad (1)$$

where k_e is the appropriate escape rate constant. The B/R values were measured relative to a "base line" where both supply lines (through the reactor and the bypass) were closed.

Because of the low volatility of diphenylmethane and 2-benzyl- and 4-benzylpyridine, a separate little Knudsen cell, which could be independently heated, served as the souce of feed gas. The design and dimensions of the all-quartz reactor have been given in ref 9. The Knudsen cell on top of the main reactor was encased in an aluminum block that was heated by two cartridge heaters under the control of a temperature control unit. The main reactor was resistively heated by clam-shell heaters; the transfer lines were heated by means of sticky heating tape. The temperature was monitored with the aid of Chromel-alumel thermocouples (referenced to 0 °C) at five locations (1, inlet line; 2, center well of reactor; 3, reactor wall; 4, bypass line; and 5, aluminum block oven). The bypass line was heated directly by sticky filament tape (as were all the inlet lines), but was always found hotter than the inlet lines because of its proximity to the clam-shell heater of the VLPP reactor. As an example, for 959 °C in the VLPP reactor, position 1 was at 198 °C, 2 at 965 °C, 3 at 952 °C, 4 at 474 °C, and 5 at 97 °C. Even at the highest temperatures of the bypass line, no evidence of unimolecular decomposition in the bypass line was found in the mass spectrum of the effusing gas.

In practice, the unimolecular decomposition kinetics were determined by observing the B/R ratio of the mass-spectral signal intensity of the parent molecular ion at constant flow rate as a function of temperature (see paragraph at end of text regarding supplementary material). In the predecomposition temperature range, the data served to set up the B/R calibration line, and decomposition started above 1000 K. The flow rate was determined by observing the static pressure in the VLPP reactor by means of an absolute pressure transducer (Baratron MKS no. 227 AHS-A1). The pressure rise was reproducible only with the large aperture in place, i.e., at lower pressures. With the small aperture, long-lasting memory effects were discernible.

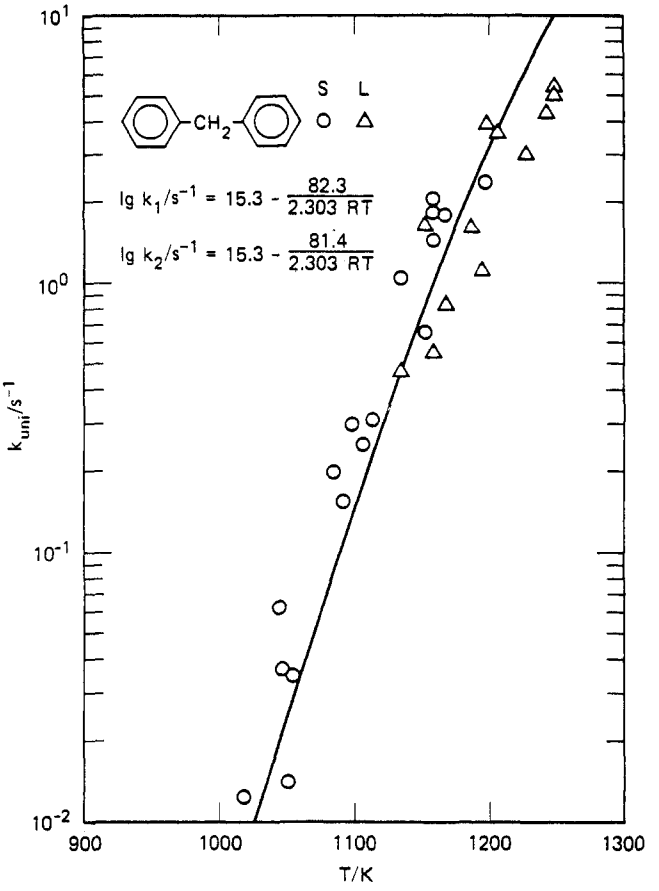

Figure 1. VLPP data for unimolecular decomposition of diphenylmethane, and RRKM calculation (solid line) of the total rate of disappearance in terms of the indicated high-pressure Arrhenius parameters. k_1 corresponds to the C-C bond scission process and k_2 corresponds to the C-H bond scission process.

The chemicals were the highest grade commerically available: diphenylmethane (Aldrich) and 2-benzyl- and 4-benzylpyridine (Aldrich). They were introduced as a liquid in the Knudsen cell without further purification.

Results and Discussion

Reaction Mechanisms and Products. Pyrolysis of diphenylmethane under VLPP conditions is expected to occur according to the following initial reactions (masses in amu are in parentheses):

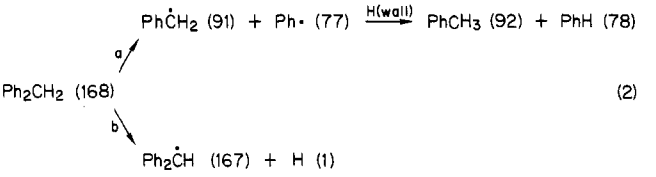

(2)

The mass spectrum of diphenylmethane shows high-intensity peaks at m/e 165, 167, and 168, corresponding to $(M - 3)^+$, $(M - 1)^+$, and M^+. For monitoring the unimolecular decomposition kinetics, the decrease in m/e 168 was observed as a function of temperature and thus corresponded to the total loss of diphenylmethane, i.e., to the sum of both decomposition pathways shown in eq 2.

To detect the reaction products and to measure the branching ratio of C-C vs. C-H bond scission processes, we monitored the mass-spectral intensity of m/e 77, 78, 79 and m/e 91, 92, 93 at elevated temperatures, where sizable decomposition occurred for the parent compound flowing through the VLPP reactor. The "bypass mass spectrum", i.e., undecomposed diphenylmethane,

(9) McMillen, D. F.; Trevor, P. L.; Golden, D. M. *J. Am. Chem. Soc.* **1980**, *102*, 7400. Ogier, W.; McMillen, D. F.; Golden, D. M. *Int. J. Chem. Kinet.*, in preparation.

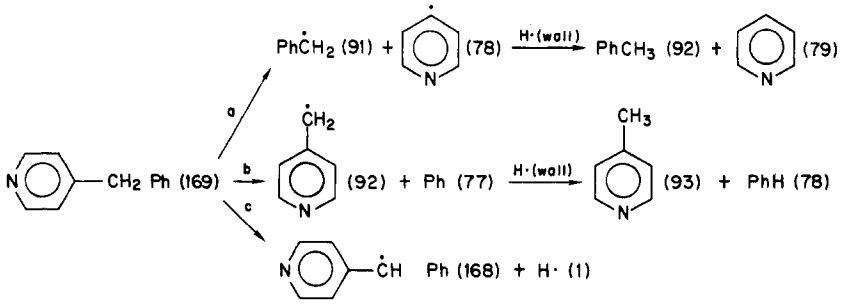

(3)

showed a sizable peak at m/e 77, small intensities at m/e 78 and an even smaller contribution at m/e 79. The same situation held for m/e 91 (large) and m/e 92 (small). At 850 °C with flow through the reactor, m/e 78 and 92 increased dramatically, and m/e 91 increased to a lesser extent, indicating production of benzene and toluene and smaller amounts of benzyl radical. The mass spectrum at m/e 165, 167, and 168 also changed significantly; the m/e 165 peak due to diphenylmethyl radical became stronger at the expense of m/e 167 and 168. At 900 °C we noted a further decrease in m/e 77, a continued increase in m/e 78, and a similar increasing ratio of m/e 92 vs. m/e 91; m/e 165 has now become the dominant peak over m/e 167, 168, with m/e 166 sharply increased in the "reactor mass spectrum" with respect to the "bypass mass spectrum" (see supplementary material).

We interpret these results to mean that the branching ratio (2a)/(2b) is roughly 1:1, with the limits being 1:2 to 2:1, because the buildup of benzene (m/e 78) and toluene (m/e 92) occurs concomitantly with the change in the spectrum at m/e 165–168 (peak intensity ratios), which we interpret as corresponding to the buildup of the diphenylmethyl radical. Had the branching ratio been significantly different from 1, we should have observed the changes in the mass-spectral peak intensity ratio of 78:77, 92:91, and 165:168 at significantly different temperatures.

Phenyl radical produced in the initial homolysis is expected to rapidly abstract hydrogen atoms from the wall of the VLPP reactor (m/e 77 → 78), thereby ending up as benzene. Benzyl radical abstracts H atoms to a certain extent as evidenced by the prominent increase in m/e 92. At these temperatures, we expect a measurable steady-state concentration of benzyl radical. At 850 °C, m/e 91 showed a pronounced increase in the B/R comparison, but at 900 °C it showed less of an increase relative to m/e 92. We interpret this result to mean that at higher temperatures, benzyl radical increasingly abstracts H atoms from the wall. The temperatures attained in this study are still confortably low enough to render the unimolecular decomposition of benzyl radical insignificant.[7]

For 4-benzyl- and 2-benzylpyridine, the expected reaction mechanism is very similar to the corresponding one in diphenylmethane, except that in this case there are two different (competing) C–C bond homolysis processes. This is illustrated in eq 3.

At temperatures where unimolecular decomposition takes place (900 °C), we observe a dramatic increase of mass-spectral intensity at m/e 78 and a new peak at m/e 79 in our B/R comparison of 4-benzylpyridine. The same situation holds for m/e 92, and m/e 93 is newly observed. The peak intensity ratios at m/e 167, 168, and 169 changed significantly at decomposition temperatures, with m/e 167 being the strongest with a concomitant increase at m/e 166. At low temperatures, however, m/e 169 (parent molecular ion) was highest in intensity. We take the increase in m/e 78, 79, 91, and 92 to indicate the formation of all four hydrogenated products from reaction 3a,b. We expect the two phenyl radicals to rapidly abstract a hydrogen atom from the walls of the reactor, thus leading to benzene and pyridine. The benzylic radicals are expected to be stable to some extent (molecular ions at m/e 91 and 92) with increasing H-abstraction activity at higher temperatures (molecular ions at m/e 92 and 93), analogous to the diphenylmethane case (cf. above).

It is clear that a precise assessment of the branching ratio (eq 3a,b) is not possible with the present technique. We expect the branching ratio to be close to unity in view of the rather similar C–C bond homolysis processes involved here and with diphenylmethane. Qualitatively, this expectation is borne out; that is, the branching ratio is close to unity at 900 °C because of the concerted change with increasing temperature of the mass spectrum in the region of the parent ion (m/e 165–169), of the (aza)benzene (m/e 77–79), and of the (aza)toluene (m/e 91–93). The same conclusions are also valid for 2-benzylpyridine, which shows minor differences in its mass spectrum compared with 4-benzylpyridine.

In conclusion, we observe all the diphenylmethanes to begin to decompose at 800 °C in the small-aperture VLPP reactor, with branching ratios of approximately unity over the accessible temperature range.

Unimolecular Decomposition Kinetics and RRKM Falloff Calculations. The decomposition kinetics were measured by observing the B/R ratio of the mass-spectral signal intensities of the parent molecular ion as a function of temperature, according to eq 1. Thus, for diphenylmethane, m/e 168, and in the case of 2-benzyl and 4-benzylpyridine, peaks at m/e 169 were monitored at unit mass resolution. The measured unimolecular decomposition rate constants k_{uni}, therefore, correspond to the sum of all decomposition pathways, namely, eq 2a,b and 3a–c, and are displayed in Figures 1 and 4 as a function of temperature.

The data, although somewhat scattered, are nevertheless noteworthy in that they represent the one and only VLPP study where a gas-phase homogeneous C–H bond-breaking process has been successfully studied. (The scattered data are the results of difficult conditions imposed by the substrate volatility limits and of a low sensitivity obtained with a small ($^3/_8$in. rods) quadrupole which was all that was available for this experiment at the time.) All previous attempts at directly measuring C–H bond dissociation energies failed, presumably due to the operation of rapid chain reactions involving H atoms. The absence of fast H-atom chain reactions is indicated by the absence of significant flow rate dependence and by the agreement between rate constants determined by using the large and small apertures, where the relative rates of unimolecular and bimolecular reactions vary by 2 orders of magnitude. The absence of fast-atom chain reactions could be related to the wall conditions in the VLPP. In this scenario, the high gas-phase hydrocarbon concentration at high temperatures leads to continuous "activation" of the VLPP reactor walls such that a sizable gas-phase H-atom concentration cannot build up because of H trapping by the reactor walls. As noted above, the flow rates of diphenylmethane into the VLPP reactor were high and varied between 4×10^{16} and 5×10^{16} molecules/s, corresponding to a temperature of 80–82 °C of the Al-block oven heating the Knudsen cell on top of the VLPP reactor. The flow rates for 2-benzyl and 4-benzylpyridine were not measured with the capacitance manometer. Assuming equal sensitivities of the parent molecular-ion peaks, these flow rates were comparable to Al-block temperatures about 20 °C higher than those for diphenylmethane, in accordance with the respective boiling points.

The flow-rate dependence of k_{uni} in the small-aperture reactor amounted to an increase of approximately 40% on increasing the flow rate of diphenylmethane 6.3-fold at 886 °C. This systematic increase was deemed insignificant in view of the experimental scatter of k_{uni} (cf. Figure 1), which is close to a factor of 2. The flow-rate variation of k_{uni} in the large-aperture reactor at 973 °C amounted to approximately 10% and did not show any systematic

trend over a variation of a factor of 9.3 in flow rates. Thus, we conclude that k_{uni} does not depend significantly on the flow rates used in the present study for both the large- and the small-aperture setting of the VLPP reactor.

Every molecule whose unimolecular decomposition has been studied by the VLPP method was found to be in the pressure "falloff" region of its unimolecular decomposition. The present molecular systems are no exception, even though they are at the upper end of the complexity of molecular systems amenable to study the VLPP. The extent of the unimolecular falloff as measured by k/k_∞ for diphenylmethane varied from 0.83 and 0.78 at 1050 K to 0.48 and 0.43 at 1250 K for reactions 2b and 2a, respectively.

As discussed in the literature many times before, there is no unique set of Arrhenius parameters describing the temperature dependence of k_{uni}, so it is not possible to "prove" a given set of Arrhenius parameters in the absence of supportive high-pressure data (at a different temperature), usually from static experiments at high total pressure. Therefore, we adopt the method of making an educated guess of the A factor and fit the falloff data with the "best" activation energy by calculating the falloff rate constant, k_{uni}, by the RRKM method, which has been adapted to describe the two-channel reaction system (eq 2a,b).

Following this procedure, the activation energy for C–H bond homolysis (reaction 2b) is determined as follows. For the C–C bond homolysis process in diphenylmethane (reaction 2a), we assume log A/s^{-1} = 15.3 (in analogy to the C–C bond scission in ethylbenzene to yield and methyl radicals[2]). From the known heats of formation of the radicals,[1] a bond dissociation energy (BDE) at 300 K of 86.7 kcal mol^{-1} can be computed, thus resulting in an activation energy of 82.3 kcal mol^{-1} at T = 1200 K using the suggested "universal" relationship between activation energy and BDE for a bond scission process (ref 1). With this choice of parameters for reaction 2a, k_{uni} is determined by the kinetic parameters of reaction 2b whose A factor we assume to be equal to the corresponding one in reaction 2a. This A factor corresponds to $\Delta S^\ddagger$ = 6.7 cal K^{-1} mol^{-1} (eu) at 1200 K and may seem high for a transition state leading to dissociation of a C–H bond, especially in comparison with a corresponding C–C bond-breaking process involving two large fragments (phenyl and benzyl radical, reaction 2a). However, the recombination rate constant (reverse of reaction 2b) is at the upper range of the expected magnitude (see below), so that we may look upon log A_b = 15.3 as an upper limit for reaction 2b. Armed with the kinetic parameters of reaction 2a and an A factor of 2×10^{15} s^{-1} for reaction 2b, we find an activation energy of 81.4 kcal mol^{-1} for reaction 2b by fitting the sum of both rate constants to the experimental values of k_{uni} as a function of temperature (Figure 1).

The molecular frequencies and moments of inertia of the transition-state model for both decomposition pathways are provided as supplementary material (Table A-1). All the hindered internal rotations have been treated as low-frequency vibrations leading to two 30-cm^{-1} vibrations at T = 1200 K for the C–Ph internal rotation (2 kcal mol^{-1} barrier) for the molecule. Because of the high temperature the entropy decrease due to the presence of the small barrier is negligible (0.1 eu), and the rotation is essentially unhindered. In the transition state leading to C–C bond rupture (reaction 2a), the free rotation of the phenyl fragment was represented by a 30-cm^{-1} vibration, whereas the Ph–$\dot{C}H_2$ hindered internal rotation was treated as a 350-cm^{-1} vibration at 1200 K due to resonance stiffening (12 kcal mol^{-1} barrier, i.e., 10 kcal mol^{-1} resonance contribution and 2 kcal mol^{-1} nonbonded interaction as in propylene assuming additivity of the various barriers). In the transition state leading to C–H bond scission (reaction 2b), the two C–Ph hindered rotations were described by a 45- and a 60-cm^{-1} vibration corresponding to a barrier to internal rotation of 12 and 6 kcal mol^{-1}. The value of the lower barrier to rotation of 6 kcal mol^{-1} for the second phenyl ring results from a comparison of the C–CH_3 bond strengths in 1,1-diphenylethane[8] (see below) and isopropylbenzene,[2] or of the C–H bond strenghs in diphenylmethane and ethylbenzene (Table II) indicating that the substitution of a methyl group by an additional phenyl ring causes an additional 4 kcal mol^{-1} resonance stabilization energy in a diphenylmethyl-type radical.

As noted in the Introduction, Troe and co-workers proposed substantially higher Arrhenius parameters for toluene decomposition near the high-pressure limit[7] than the consensus values for both the activation energy and A factor. These higher values appear questionable in view of the much higher temperatures used in shock-tube studies, but because of the limited literature data for C–H bond scissions and the ambiguities involved in the conversion of high-temperature kinetic data to ΔH°_{298} values, they cannot be rejected out of hand. Therefore, to help resolve the discrepancy, we attempt to predict the kinetic parameters for diphenylmethane decomposition on the basis of the Troe parameters for toluene (cf. introduction of the C–H bond-breaking step, reaction 2b) by making appropriate corrections for A factor and activation energy.

The decrease of the entropy of activation for introducing an additional phenyl ring with a 6 kcal mol^{-1} barrier to internal rotation amounts to approximately −0.3 eu at 1200 K, thus reducing the A factor from 16.9 to 16.8 logarithmic units. Furthermore, in going from toluene to diphenylmethane, there is a reduction in reaction path degeneracy from 3 to 2, thus lowering log A to 16.6. A reasonable estimate for the activation energy involves subtraction of 3.0 kcal mol^{-1} for the shift of primary (toluene) to secondary C–H bond (in diphenylmethane) and an additional subtraction of 4.0 kcal mol^{-1} due to additional resonance stiffening in the second phenyl ring upon C–H bond rupture in diphenylmethane, thus leading to an activation energy of roughly 84.0 kcal mol^{-1} for reaction 2a:

$$\log k/s^{-1} = 16.6 - 84.0/(2.303RT) \qquad (4)$$

When we compute the unimolecular rate constant for our VLPP conditions for reaction 2a using the given high-pressure Arrhenius parameters of eq 4 and the two-channel RRKM model, we find that the Troe parameters lead to a value of k_{uni} about a factor of 3 higher than our measured ones over the temperature range 1050–1200 K. These absolute rate constants are significantly higher than the experimental values presented in Figure 1, although we believe our uncertainties to be close to a factor of 2. We take this result as an indication that the Arrhenius parameters for toluene decomposition are abnormally high, although the argument may be somewhat questionable given the adjustments in the kinetic parameters of toluene decomposition to accommodate diphenylmethane decomposition.

More solid support for a "low" set of kinetic parameters for the C–H bond dissociation in diphenylmethane comes from a comparison of the standard heats of formation of diphenylmethyl radical generated on one hand by C–H bond dissociation (reaction 2a, present work) and on the other hand by C–C bond dissociation in 1,1-diphenylethane (reaction 5). As shown below, these derived

$$Ph_2CHCH_3 \rightarrow Ph_2\dot{C}H + \dot{C}H_3 \qquad (5)$$

$\Delta H_f^\circ{}_{300}$ are 68.0 and 69.0 kcal mol^{-1}, respectively, but use of the high A factor proposed by Troe[7] for the C–H bond scission in diphenylmethane would result in a $\Delta H_f^\circ{}_{300}$ for the diphenylmethyl radical of 72.3 kcal mol^{-1}.

We used the excellent VLPP data of Robaugh[8] on 1,1-diphenylethane decomposition (Figure 2), and to obtain a consistent set of kinetic parameters based on similar transition-state models for both types of bond fission reactions, we performed single-channel RRKM calculations on the unimolecular decomposition of 1,1-diphenylethane (Figure 2), reaction 5, and 2,2-diphenylpropane (Figure 3), reaction 6. Because of the different nature

$$Ph_2C(CH_3)_2 \rightarrow Ph_2\dot{C}CH_3 + \dot{C}H_3 \qquad (6)$$

of the bond scission processes (C--C vs. C--H), the temperatures at which the kinetic parameters were estimated vary slightly. In reducing activation energies to bond dissociation energies, we took into account these differing temperatures (see below). The A factor for reaction 5 was estimated to be 15.4 logarithmic units at 1000 K based on the A factor CH_3–C bond fission in isopropylbenzene (log A/s^{-1} = 15.8), which has been corrected for

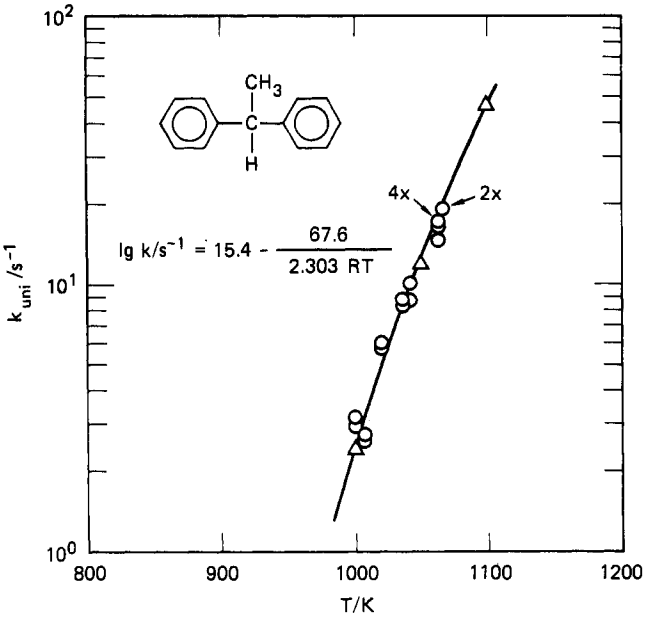

Figure 2. VLPP data of Robaugh[8] for unimolecular decomposition of 1,1-diphenylethane and RRKM calculation (solid line) of the C--CH_3 bond scission process in terms of the indicated high-pressure Arrhenius parameters.

reaction path degeneracy of unity (Δ log A = −0.3) and for additional resonance stiffening of 4.0 kcal mol^{-1} in view of the presence of the second phenyl ring (Δ log A = −0.1). This additional stiffening is that expected for a barrier to internal rotation of 6 kcal mol^{-1} in analogy to the situation in diphenylmethane decomposition (see above). Here we compare the barrier to internal rotation of C–Ph in 1,1-diphenylethane to the barrier of C–CH_3 rotation in isopropylbenzene, whose net difference is 4.0 kcal mol^{-1}. The next paragraph elaborates on the distinction of rotational barrier vs. resonance contribution to that barrier. A closer look at this problem is necessary to make the thermochemical and kinetic parameters consistent with each other when different precursors are used to obtain the same radical.

In the diphenylmethane decomposition to diphenylmethyl radical and H·atom (reaction 2b), the adjustment of the A factor was taken relative to the one for toluene decomposition (see above), which means a net increase in the rotational barrier of 6 kcal mol^{-1} due to the absence of internal rotation of a C–H bond. However, in assessing the A factor for C–C bond scission in 1,1-diphenylethane (reaction 5), we take the corresponding A factor for isopropylbenzene decomposition as a standard that already includes a barrier to C–CH_3 internal rotation of 2–3 kcal mol^{-1}. Hence, the net effect of the resonance stabilization due to the second phenyl ring in the 1,1-diphenylethane transition state is believed to amount to 4 kcal mol^{-1} relative to the analogous process in isopropylbenzene when based on C–H bond dissociation processes. In the interest of brevity, we refrain from describing the transition-state parameters of 1,1-diphenylethane in detail at this point. Instead, we point to Table A-2 (supplementary material) for a complete list of molecular and complex parameters and add that the same barriers to internal rotation—mutatis mutandis—were used as in diphenylmethane decomposition, reaction 2b.

The fit to Robaugh's experimental data[6] is shown in Figure 2 together with the limiting high-pressure Arrhenius expression as computed by a standard RRKM calculation. The point we would like to stress here is that the resulting activation energy of 67.6 kcal mol^{-1} at 1000 K leads to a standard heat of formation at 300 K for diphenylmethyl radical of 68.0 kcal mol^{-1} compared with $\Delta H_f°_{300}$ of 69.0 kcal mol^{-1} for diphenylmethyl from C–H bond scission in diphenylmethane (Tables I and II). We take this excellent agreement of $\Delta H_f°$ for diphenylmethyl radical derived from two different reaction pathways leading to the same radical as coorborating evidence that there is nothing abnormal in the Arrhenius parameters of a C–H bond dissociation process compared to a normal C–C bond-breaking process, contrary to the claim of Astholz et al.[7] We are therefore led to believe that the low set of Arrhenius parameters (see above) adequately describes the two decomposition pathways in diphenylmethane, reaction 2.

TABLE I: Summary of Kinetic Parameters[a]

molecule	$\Delta H_f°$ [a]	$\langle T \rangle$ [b]	log A [c]	E_d [d]	ref
PhCHPh	(39.7)	1200	15.3	81.4	this work
$PhCH_2$–Ph	(39.7)	1200	15.3	82.3	this work
PhCHC$_5$H$_4$N	[e]	1200	15.3	82.3	this work
$PhCH_2$–C$_5$H$_4$N	[f]				
PhCHPh	(32.8)	1000	15.4	67.6	8
Ph–C(CH$_3$)Ph	(26.4)	1000	15.8	66.2	8
Ph–CCH$_3$ (H)	(0.10)	1000	15.8	71.3	2

[a] The numbers in parentheses are $\Delta H_f°$ values in kcal mol^{-1} for the radical precursors, calculated by using Benson's group additivity tables. [b] Average T/K. [c] In s^{-1} at $\langle T \rangle$. [d] In kcal mol^{-1} at $\langle T \rangle$. [e] 2-Benzyl- and 4-benzylpyridine. [f] Parameters averaged for both pathways. [g] In converting the kinetic parameters to thermochemical quantities, $\Delta H_f°(CH_3) = 35.1$, $\Delta H_f°(C_6H_5) = 78.6$, and $\Delta H_f°(C_7H_7) = 47.8$ kcal mol^{-1} were used.

TABLE II: Bond Dissociation Energy and Radical Heats of Formation

$\Delta H_f°$(R)[a]	R	DH-(R–H)[a]	DH-(R–CH_3)[a]	ref
69.0	Ph_2CH	81.4	71.3	this work
68.0	Ph_2CH	80.4	70.3	8
b	PhCHC$_5$H$_4$N	82.3		this work
60.8	Ph_2CCH_3	80.1	69.5	8
39.6	$PhCHCH_3$	84.7	73.8 74.6[c]	2

[a] In kcal mol^{-1}. [b] Insufficient data on $\Delta H_f°$ of parent compound to compute other values. [From this work we also know DH-($PhCH_2$–C$_5$H$_4$N) = 86.7 kcal mol^{-1}.] [c] Our analysis of data (ref 2).

To further check the consistency of the kinetic parameters of methyl-substituted diphenylmethanes, we also fit Robaugh's data on 2,2-diphenylpropane to high-pressure Arrhenius parameters calculated by the RRKM method.[6] We assumed an A factor of 15.8 logarithmic units for reaction 6, based on the A factor for *tert*-butylbenzene decomposition,[2] and then adjusted for phenyl substitution analogous to 1,1-diphenylethane (cf. above). The fit is displayed in Figure 3, and the details of the molecular parameters for the transition state and the molecule are displayed in Table A-3 (supplementary material). Because these parameters are very similar to those for 1,1-diphenylethane, we will forego an extensive discussion. The fitted activation energy for reaction 6 is 66.2 kcal mol^{-1} at 1000 K (Figure 3), which leads to a C–CH_3 bond strength of 69.5 kcal mol^{-1} compared with an average of 70.8 kcal mol^{-1} for 1,1-diphenylethane (Tables I and II). This decrease of 1.3 kcal mol^{-1} in C–C bond strength upon methyl substitution is slightly smaller than the analogous change in the saturated hydrocarbon manifold ($(CH_3)_2CH$–/–CH_3 → $(CH_3)_3C$–/–CH_3 difference is 1.6 kcal mol), presumably because the phenyl-substituted system represents a stabilized system in which substituent effects and the bond strengths are attenuated.

Finally, our VLPP results on 2-benzyl and 4-benzylpyridine (reaction 3) were treated in the same manner as the diphenylmethane decomposition data by assuming the same A factors for all three decomposition channels, by lumping the two different C–C bond scission pathways together (reactions 3a and 3b), and by assigning them the same activation energy as in diphenylmethane decomposition. The fit to the data is displayed in Figure

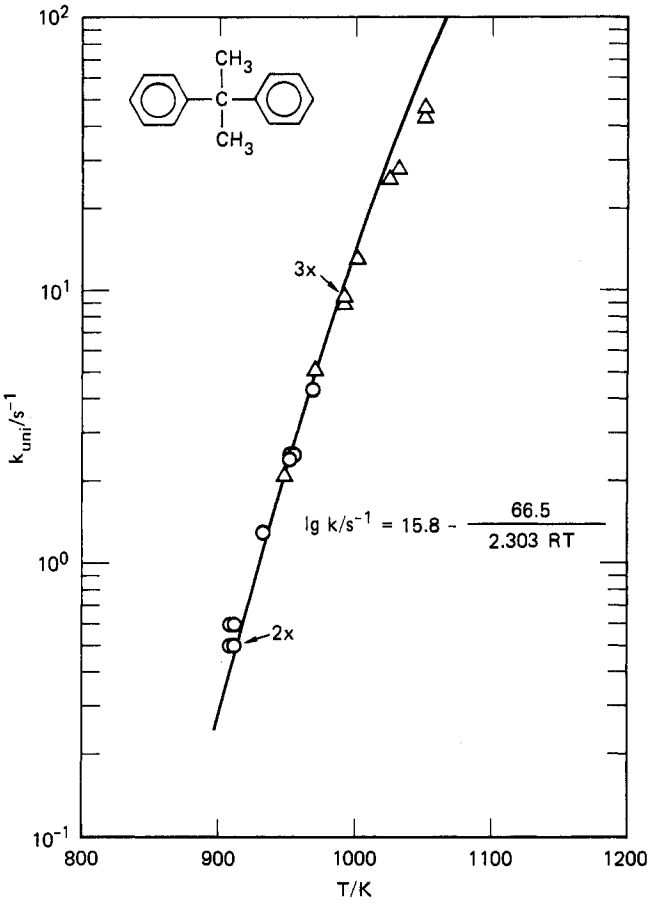

Figure 3. VLPP data of Robaugh[8] for unimolecular decomposition of 2,2-diphenylpropane, and RRKM calculation (solid line) of the C--CH_3 bond scission process for the indicated high-pressure Arrhenius parameters.

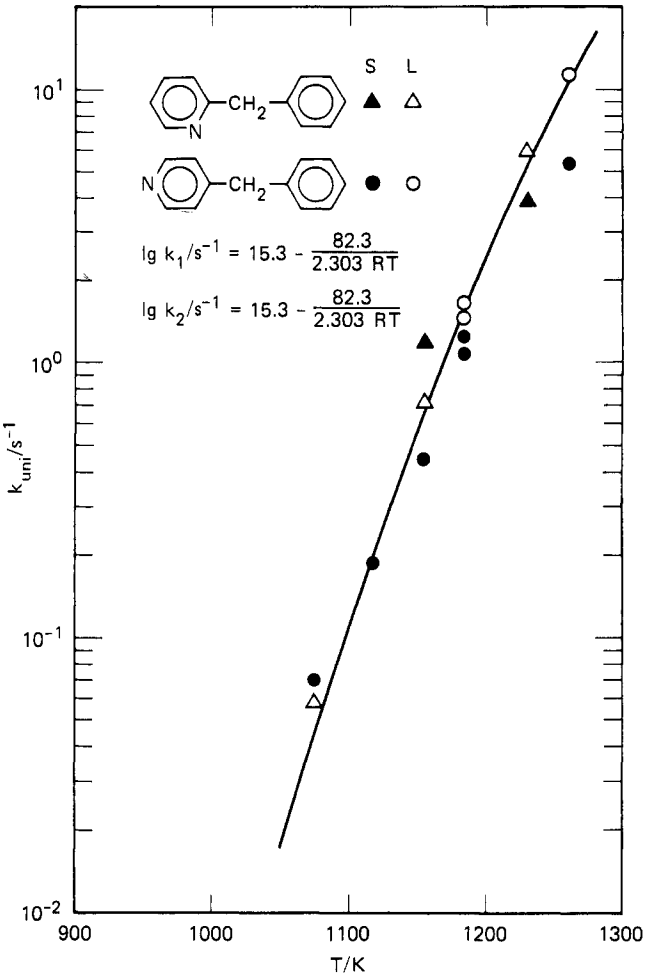

Figure 4. VLPP data for unimolecular decomposition of 2-benzyl- and 4-benzylpyridine, and RRKM calculation (solid line) of the total rate of disappearance in terms of the indicated high-pressure Arrhenius parameters; k_1 corresponds to both C–C and k_2 to the C–H bond scission processes.

4 and leads to a C–H bond strength slightly higher (by 0.9 kcal mol^{-1}) with respect to the same C–H bond in diphenylmethane (Table II) using the same transition-state parameters as for diphenylmethane (Table A-1). This corresponds very closely to the 1.7 and 1.0 kcal mol^{-1} higher BDEs measured for 2-ethyl- and 4-ethylpyridine by Barton and Stein.[10] In view of the complexity of the molecular system and its decomposition pathways, the statement of significance is that aza substitution in one of the phenyl rings leads to a decomposition slower by 25% at 1200 K with respect to the unsubstituted system. The kinetic parameters for the discussed systems are shown in Tables I and II along with the thermodynamic parameters that will be discussed in the next section.

Bond Strengths Derived from Bond Fission Activation Energies. Making the frequently used assumption that radical–radical recombination reactions have no activation energy at some temperature and with a given measure of number density (pressure or concentration units), we can now convert the activation energy for bond fission to the thermodynamic parameter of bond strength. We adopt the convention outlined in ref 1 that there is no activation energy for radical–radical recombination at 0 K when the number density is expressed in molar units and when the Gorin rotational transition-state model is used for bond dissociation processes. With these assumptions, the relationship between the Arrhenius activation energy $E_{T,d}$ at temperature T and the bond strength (BDE) in question, i.e, the enthalpy of the bond dissociation reaction at 298 K ($\Delta H°_{298}$), assumes the following form:

$$\text{BDE} = \Delta H°_{298} = E_{T,d} - \langle \Delta C_p° \rangle_{298}^{T}(T - 298) + \tfrac{1}{2}RT \qquad (7)$$

where $\langle \Delta C_p° \rangle_{298}^{T}$ is the average heat capacity of the reaction in question over the temperature range 298–T K.

TABLE III: Heat Capacity Changes as a Function of Temperature for Reactions Listed in the Text

reaction	$\langle \Delta C_p \rangle^a$ 450 K	500 K	750 K	850 K	1050 K	$E_{T,d}$ – BDE[b]
2a	−3.47		−3.65		−3.61	−4.42
2b	1.82		1.54		0.72	0.02
5		−2.14		−2.30		−2.60
6		−3.40		−3.12		−3.30
8		−2.95		−3.57		−3.25

[a] ΔC_p in units of cal K^{-1} mol^{-1}. [b] T = 1200 K for reactions 2a and 2b; T = 1000 K for reactions 5, 6, and 8. Units of kcal mol^{-1}.

Table II presents values for C–H and C–C bond dissociation energies leading to diphenylmethyl radicals using eq 7. The difference terms $E_{T,d} - \Delta H°_{298}$ for the various reactions are displayed in the last column of Table III and have been calculated by using reasonable assumptions regarding the molecular structure of reactants and products. In these calculations only those few modes that changed the most in going from reactant to product have been considered. We also found that the barriers to internal rotation (V_{ir}) determined to a considerable extent the magnitude of the above difference terms, despite the high temperatures.

In what follows we give a brief account of V_{ir} for the different combinations of reactants and products: in calculating $E_{T,d} - \Delta H°_{298}$ for reaction 2a (C–C bond fission), we assigned V_{ir} = 2 kcal mol^{-1} to both of the C–Ph rotations in diphenylmethane, whereas V_{ir} = 12 kcal mol^{-1} was used for benzyl radical. For the

(10) Barton, B. D.; Stein, S. E. *J. Chem. Soc., Faraday Trans. 1* **1981**, *77*, 1755.

diphenylmethyl radical generated in reaction 2b, V_{ir} = 12 and 6 kcal mol^{-1} were used in accordance with the results (from Table II) that the additional resonance stabilization associated with the second phenyl ring in diphenylmethyl radical (as compared to the 1-phenylethyl radical) amounts to 4 kcal mol^{-1}, as discussed above.

The interesting conclusion from the comparison of the C–C and the C–H bond dissociation difference terms, $E_{T,d} - \Delta H°_{298}$, in the last column of Table III is that for the C–H process, BDE $\cong$ $E_{1200,d}$, whereas for the C–C process there is a sizable difference term (−4.4 to −2.6 kcal mol^{-1}) over the stated temperature range, resulting from a substantial negative heat capacity change at high temperatures for C–C bond scission. In an analogous manner, 1,1-diphenylethane decomposition (reaction 5) was analyzed in terms of V_{ir} = 2 × 2(C–Ph) + 3(C–CH_3) kcal mol^{-1} for the molecule, and 2,2-diphenylpropane was assigned V_{ir} = 2 × 2(C–Ph) + 2 × 3(C–CH_3) kcal mol^{-1} for the molecule and V_{ir} = 12(C–Ph) + 6(C–Ph) + 2(C–CH_3) kcal mol^{-1} for the resulting radical in reaction 6. To derive the set of bond strengths in a consistent manner, we analyzed the data for reaction 8 using the

$$PhCH(CH_3)_2 \rightarrow PhĊHCH_3 + ĊH_3 \qquad (8)$$

analogous molecular parameters, namely, V_{ir} = 2 × 3(C–CH_3) + 2(C–Ph) kcal mol^{-1} for isopropylbenzene and V_{ir} = 12 + 2 kcal mol^{-1} for the resulting 1-phenylethyl (or α-phenethyl) radical from reaction 8. In adhering to the above-mentioned convention, eq 7, we deduce a C–C bond strength of 74.6 kcal mol^{-1}, whereas Robaugh's treatment of his data led to BDE = 73.8 kcal mol^{-1}, which is not significantly different from our analysis (cf. Table II). The difference of 4 kcal mol^{-1} in the BDE of isopropylbenzene and diphenylmethane corresponds to the phenyl-substitution effect of phenyl-substituted methanes (cf. Table II), whereas the methyl-substitution effect in the diphenylmethane series amounts to 0.8 or 1.3 kcal mol^{-1} if one replaces a hydrogen atom by a methyl group when considering the C–H and C–CH_3 bond dissociation process from Table II. This effect amounts to an insignificant 0.8 kcal mol^{-1} on the basis of the C–H bond scission process, which is customarily used to calculate substitution or stabilization effects in bond strengths. Both values for the effect of the above substituents agree with the values from the literature, which, as cited in a recent review,[1] were based largely on a preliminary analysis of the data of Robaugh and Stein.[8a] It thus appears that the decrease in bond strength upon methyl substitution is much attenuated in a molecular system that is already resonance stabilized.

One last remark concerns the magnitude of the rate of recombination, i.e., the reverse of reactions 2a and 2b. By assuming an A factor (of 15.3 logarithmic units) for eq 2a and 2b we can calculate k_{-2a} and k_{-2b} if one knows the reaction entropy $\Delta S°_{2a}$, $\Delta S°_{2b}$ at reaction temperature (1200 K) and the reaction enthalpy $\Delta H°_{2a}$, $\Delta_H°_{2b}$, which are easily deduced from Table II (DH° ≡ $\Delta H_r°$ at 300 K) and Table III ($\langle \Delta C_p \rangle$ values). We estimated $\Delta S°_{2a}$ = 37.33 eu, $\Delta S°_{2b}$ = 30.0 eu at 300 K from group additivity tables making appropriate corrections for the diphenylmethyl radical, and $\Delta S°_{2a}$ = 32.4 eu, $\Delta S°_{2b}$ = 32.1 eu at 1200 K using the $\langle \Delta C_p \rangle$ values of Table III (standard state: 1 atm). With $\Delta H°_{2a}$ = 83.5 and $\Delta H°_{2b}$ = 82.6 kcal mol^{-1}, log k_{-2a} = 10.4 and log k_{-2b} = 10.5 was found at 1200 K, when k is expressed in molar units. Those recombination rate constants seem rather high, but this may either be the consequence of the choice of the A factor for C–H and C–C bond dissociation, which at $10^{15.3}$ s^{-1} is believed to be at its upper limit (see abve, discussion of $\Delta S^{\ddagger}$), or be due to the inaccurate estimate for $\Delta S°_{2a}$ and $\Delta S°_{2b}$. It appears, then, that the test for reasonable recombination rate constants and the requirements of the dual precursor–single product radical (diphenylmethane C–/–H and 1,1-diphenylethane C–/–CH_3 bond scission) places an upper limit to the A factor for reaction 2b of 15.3 logarithmic units, which is 1.5 powers of 10 lower than the recently measured A factor for toluene decomposition.[7]

Correlation of Experimental Bond Strengths with First-Order PMO Energies. Many thermodynamic, spectroscopic, and kinetic parameters of planar–conjugated π-electron systems can be readily correlated (scaled) with simple one-electron MO theories of the Hückel type (zero-overlap theories).[11] The situation becomes particularly simple if one considers the interaction of two odd alternant hydrocarbon fragments, in which case a simple first-order perturbational treatment leads to relative interaction energies ΔE. These ΔE values can then be used to scale observable quantities that should depend on ΔE, such as activation energies and thermochemical parameters (enthalpies).[12,13]

TABLE IV: Experimental Bond Dissociation Energies and Nonbonding Molecular Orbital Coefficients for the Radicals Displayed in Scheme I

	BDE,[a] kcal mol^{-1}	a_{NBMO}
1	88	0.756
2	85.1	0.666
3	81.8	0.534
4	85.1	0.670
5	86.3	0.707
6	81.0[b]	0.577
7	83.0[c]	0.577
8	84.0[b]	0.632
9	85.3[b]	0.707
10	84.0[c]	0.632
11	76.0[b]	0.450
12	79.3[b]	0.632

[a] Experimental values from ref 1 and this work. [b] Corrected by +3 kcal mol^{-1} for secondary → primary C–H. [c] Based on[1]

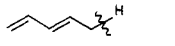

In the present case, we will treat the reverse of the C–H bond scission reaction (recombination) in conjugated, planar hydrocarbons (eq 9) in terms of the interaction of the nonbonding

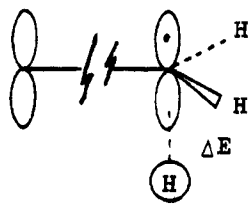

(9)

molecular orbital (NBMO) at the appropriate carbon center with the hydrogen's 1s atomic orbital. Radical recombination reactions do not have an intrinsic activation energy, so the electronic interaction of the π-NBMO with the H 1s orbital should reflect the exothermicity of the radical combination reaction, i.e., the strength of the bond formed in the reaction. Relative C–H bond strengths in the conjugated hydrocarbons correspond to relative perturbation stabilization energies in the interacting radical–hydrogen pair. ΔE thus describes the incipient interaction in that pair, which we will regard as proportional to the bond strength at the equilibrium internuclear distance, i.e., *after* the completion of the radical recombination reaction including electronic reorganization. The first-order interaction energy ΔE is given by eq 10

$$\Delta E = 2C_{R\cdot}C_{H\cdot}\gamma_{RH} \qquad (10)$$

where $C_{R\cdot}$ and $C_{H\cdot}$ are the eigenvector coefficients of the NBMO at the appropriate positions in the molecular frame and γ_{RH} is the interaction integral for the H 1s···$C_{p\pi}$ interaction. In a homologous series, e.g., Ṙ···Ḣ, interaction with different R·, γ_{RH} and $C_{H\cdot}$ (=1.0) stay constant, so that $C_{R\cdot}$ is proportional to ΔE. The NBMO coefficients $C_{R\cdot}$ depend only on the molecular topology of the radical R· and can be obtained either by inspection (in simple cases) or by the zero-sum rule in more complex radicals.[11] Table IV lists those coefficients as well as the relevant experimental bond strengths from a recent compilation[1] and from

(11) Heilbronner, E.; Bock, H. "Das HMO-Modell und seine Anwendung"; Verlag Chemie: Weinheim, 1968; Chapters 10–12.
(12) Herndon, W. C. *J. Chem. Educ.* **1979**, *56*, 448 and references therein.
(13) Herndon, W. C. *J. Org. Chem.* **1981**, *46*, 2119–25.

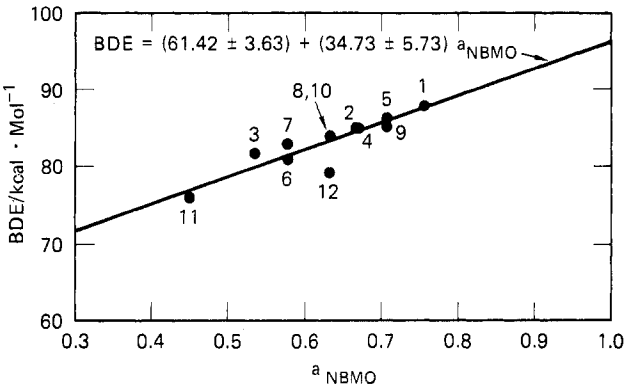

Figure 5. Correlation plot of the C–H bond dissociation energy vs. the (singly occupied) nonbonding MO coefficient at the position of bond rupture for odd alternant hydrocarbons. For the odd nonalternant hydrocarbons, **9–11**, the HOMO (highest occupied molecular orbital) coefficients at the respective positions were used. The numbering of the hydrocarbon radicals is presented in Scheme I.

this work (for diphenylmethane). Figure 5 is a graphical display of the data of Table IV, which now can be used in a predictive way due to the linear nature of the correlation whose parameters are given by eq 11. Because of the extreme simplicity of the

$$\mathrm{BDE} = (61.42 \pm 3.63) + (34.73 \pm 5.73)C_{\mathrm{R}\cdot} \qquad (11)$$

concept, the BDE values had to be normalized because the model is not designed to distinguish between primary, secondary, and tertiary C–H bonds. Therefore, for the BDE values in Table IV to correspond to primary C–H bonds, a correction of +3 kcal mol^{-1} has been applied to all experimental values pertaining to secondary C–H bonds. Furthermore, in the case of the odd nonalternant hydrocarbons **10** and **11**, ΔE has been calculated also in first order (eq 10), although these radicals do not have a nonbonding molecular orbital strictly speaking. In those cases, the highest occupied molecular orbital (HOMO) is either weakly bonding (**10**) or weakly antibonding (**11**), so ΔE should be calculated in second order. However, we decided to estimate ΔE by the first-order expression, using $C_{\mathrm{R}\cdot}$ of the symmetric HOMO, because it is more than likely that the error is within the experimental uncertainty of the BDE determination.

The linear correlation of Figure 6 has two gratifying features: first, it is linear, so that predictions of C–H bond dissociation energies are easily made by using eq 11; second, for $C_{\mathrm{R}\cdot} = 1$, BDE is predicted as 96.15 kcal mol^{-1}. This situation corresponds to a primary C–H BDE where the unpaired electron resides in a NBMO that is not delocalized, i.e., in a pure p atomic orbital. This case is most easily identified with R–CH_2·. In fact, the BDE in ethane is 98 kcal mol^{-1}, a value that falls within the uncertainty of the linear extrapolation to $C_{\mathrm{R}\cdot} = 1$ according to eq 11. The extrapolation to $C_{\mathrm{R}\cdot} = 0$ is more interesting, although it is harder to identify a molecular structure of an odd alternant hydrocarbon pertaining to this case. A limiting case could be the C–H BDE of a C–H bond in graphite, leading to a π-radical with negligible electron density at the reaction center. Such a bond is predicted to have a BDE of 61.4 kcal mol^{-1}, although it is likely that other electronic effects not currently incorporated in this crude model will be of increasing importance as one approaches the limit $C_{\mathrm{R}\cdot} = 0$.

A test of the correlation in the vicinity of the lower limit might be provided by the phenalenyl system (structure **13** in Scheme I). With an NBMO coefficient of 0.4, the correlation (eq 11) predicts an adjusted (to primary C–H) BDE of 74 kcal mol^{-1}. Although there are no explicit BDE measurements of the C–H bond strength in phenalene, the ESR observation[14] of phenalenyl radical in equilibrium at room temperature with the radical dimer would appear to require an upper limit of 70 kcal mol^{-1} on the adjusted C–H bond strength. The above discrepancy is not

Scheme I

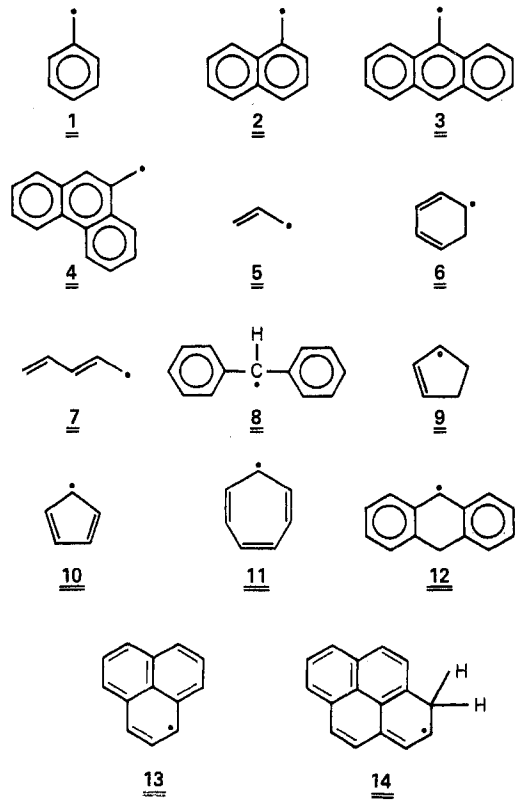

disheartening since phenalenyl radical, having $4n + 2$ electrons in each ring, is not exactly analogous to cyclohexadienyl systems. Similarly, the 1-hydropyrenyl radical (**14** in Scheme I), although a cyclohexadienyl system, is also a vinylogous phenylenyl radical and appears to exhibit unusual stability.

More pertinent to the question of the validity of the correlation in eq 11 is the 9-hydroanthryl radical (**12** in Scheme I), whose recently measured[9] bond strength of 79 kcal mol^{-1} (adjusted) puts it ~4 kcal mol^{-1} below the correlation in Figure 5. This is in contrast to the electronically equivalent diphenylmethyl radical (**8** in Scheme I and Figure 5), for which the measured value falls almost directly on the line.

The 4 kcal mol^{-1} discrepancy in experimental BDE values in fact is subject to considerable uncertainty, because of the assumption which had to be made in estimating A factors. The loss of one phenyl rotation on homolysis of 1,1-diphenylethane (reaction 5) will lower the A factor as compared to cumene (reaction 8). However, it has recently been shown[15] that in 9,10-dihydroanthracene, while there is no internal rotation as such, there are in fact large ring motions ("butterfly motions") that will make a large contribution to the entropy of most 9,10-dihydroanthracene derivatives. Because most of this entropy is lost on **9**–X bond homolysis, A factors from such homolyses would tend to be abnormally low. Unless properly accounted for, these low A factors would result in the attributing of low rates to high activation energies and thus result in incorrectly *high* BDE values. Thus, there are two competing factors which must be taken into account in converting relative homolysis rates for diphenylmethyl derivatives and 9,10-dihydroanthracene derivatives into BDE differences. The point 8 in Figure 5 reflects a correction (to lower BDE) for the rotational entropy loss in diphenylmethyl–X, but we do not yet have a fully satisfactory basis for correcting point 12 for entropy loss on account of the butterfly motion. Therefore it seems likely that, if anythin, the BDE value for 9,10-dihydroanthracene should actually be lower than shown in Figure 5. That is, the actual difference between the BDE values for diphenylmethane and 9,10-dihydroanthracene should be greater than the difference

(14) Lewis, I. C.; Singer, L. S. *Singer, L. S. Carbon* **1969**, *7*, 93–9. Reid, D. H. *Chem. Ind.* **Dec. 22, 1956**, 1504–5.

(15) Raber, D. J.; Harder, L. E. Rabideau, P. W.; Lipkowitz, K. B. *J. Am. Chem. Soc.* **1982**, *104*, 2843.

between points 8 and 12 in Figure 5.

Problems of accurate measurement of BDE values in hydroaromatic systems notwithstanding, it would seem to leave the simple NBMO approach (like the correlations of Stein[8b] and Herndon[11,12]) as an empirically useful correlation which can be used as a predictor of proven or known reliability for BDE values which are hard to measure, or for rates measured at high temperature (e.g., in shock-tube experiments) where the reduction to BDE values ($=\Delta H_r°$ at room temperature) is uncertain due to unknown heat capacities.

Conclusions

We have shown that the decompositions of the title compounds proceed, more or less equally, via two pathways, a C–C scission and a C–H bond break. Taking the C–H bond energy as the unknown, we have measured $\Delta H_f°_{298}(Ph_2\dot{C}H, g) = 69$ kcal mol^{-1}. This value indicates that the extra stabilization energy associated with replacing the CH_3 group in $Ph\dot{C}HCH_3$ with a second Ph group to form $Ph_2\dot{C}H$ is ~4 kcal mol^{-1}. We have also measured the respective bond dissociation energies in the N-substituted compounds, but cannot report a radical heat of formation because data are lacking for heats of formation of the parent compounds.

Our value of $\Delta H_f°_{298}(Ph_2\dot{C}H,g)$ agrees within less than 1 kcal mol^{-1} with that from the data of Robaugh and Stein,[8] suggesting that the A factor for the toluene C–H bond dissociation process, contrary to recent reports,[7] is comparable to those for all other benzyl–X dissociation.

Acknowledgment. We thank Dr. R. Patrick of our group for his kind help in adapting the RRKM program to the large number of oscillators used in the present study and for his assistance in performing the falloff calculations. This work is supported in part by the Department of Energy, contract no. DE-ACO3-79ER10483.

Supplementary Material Available: A table of B/R ratios and rate constants at various temperatures for unimolecular decomposition of diphenylmethane and 2-benzyl- and 4-benzylpyridine in small- and large-aperture reactors; a figure illustrating the changes in the mass spectrum of diphenylmethane at 900 °C at m/e 77, 78, 91, 92, and 165–168; and Tables A-1–A-3 listing molecular and transition-state parameters for the decomposition of diphenylmethane, 1,1-diphenylethane, and 2,2-diphenylpropane (6 pages). Ordering information is given on any current masthead page.

Spectral Analysis of the Chemiluminescence Generated by $H_3B·X + O(^3P)$

P. M. Jeffers† and S. H. Bauer*

Department of Chemistry, Cornell University, Ithaca, New York 14853 *(Received: January 9, 1984)*

In a flow tube reactor, intense chemiluminescence is generated when low pressures of $H_3B·N(CH_3)_3$ or other borane adducts are rapidly mixed with $O(^3P)$ in a He carrier. Superposed on the extended α-BO system, there are a few β-system bands, moderate intensities of OH*, NH*, CH*, and BH*, and a very strong CN*. No single vibrational temperature exists for $BO(A^2\Pi)$; the rotational temperature is 350 K.

Introduction

In a rapid-mixing fast-flow tube reactor, Anderson and Bauer[1] measured the rates of attack on B_2H_6 and $H_3B·CO$ by O and N atoms, as well as by N_2O, NO, NO_2, and O_2. The products of reaction were analyzed by a direct sampling TOF mass spectrometer. In a quartz flow tube reactor, the emitted chemiluminescence was recorded photographically. From these data both the stoichiometry and the exoergic pathways required to generate the highest recorded frequencies were determined. To account for the observations, two initiation mechanisms (which operate concurrently) were required:

mechanism 1:

$$O + H_3B·CO \rightarrow OH + [H_2BCO]^* \rightarrow OH + BH_2 + CO$$
$$\rightarrow H_2O + [HBCO]^* \rightarrow H_2O + BH + CO$$

mechanism 2:

$$O + H_3B·CO \rightarrow [H_3B·O]^* + CO \rightarrow BO + H_2 + H +$$
$$CO + \text{other compounds, with oxygen attached to boron}$$

The highly exoergic steps which generate BO* are presumed to arise from the attack by $O(^3P)$ on BH or on BH_2.

In a subsequent investigation Jeffers and Bauer[2] measured the oxidation rate of the amine–borane adducts $H_3B·N(CH_3)_3$ and $H_3B·N(C_2H_5)_3$ by O atoms. These rates are about 2 orders of magnitude faster than for borane carbonyl and 4 orders of magnitude faster than for B_2H_6. Intense chemiluminescence was again observed; when molecular O_2 was present, the flame was blue-green in color, while a cool blue flame resulted with only O atoms in the flow. The BO-α bands are the most prominent features, upon which broad fuzzy bands of BO_2 are superposed when mixtures of O/O_2 are used. In limited respects our results are similar to the reaction among $BCl_3 + O + N$, which generated $BO(X^2\Sigma^+)$ and BO_2 when O_2 was added, reported by Llewellyn et al.[3] and Sharma and Joshi who investigated $O + B(C_2H_5)_3$.[4a]

In this paper we report on detailed spectral studies of $O + H_3B·N(CH_3)_3$ and of $O + N(CH_3)_3$. We also recorded photographically spectra of the chemiluminescence emitted when $O(^3P)$ atoms were mixed, at low pressures, with borane adducts of pyridine, tetrahydrofurane, *tert*-butylamine, and dimethyl sulfide. These spectra have many features in common, associated with the BO-α band system, but each showed some unique aspects which we have not yet investigated. The emission intensities generated by the amine and the amine–borane adduct were photoelectrically recorded from 2650 to 6500 Å. The vibrational populations for the $BO^*(A^2\Pi)$ are clearly non-Boltzmannian, with some striking discontinuities in a log $N(v)$ vs. v plot (portions have

† Permanent address: Department of Chemistry, SUNY at Cortland, Cortland, NY 13045.

(1) G. K. Anderson and S. H. Bauer, *J. Phys. Chem.*, **81**, 1146 (1977).
(2) P. M. Jeffers and S. H. Bauer, *Chem. Phys. Lett.*, **80**, 29 (1981).
(3) I. P. Llewellyn, A. Fontijn, and M. A. A. Clyne, *Chem. Phys. Lett.*, **84**, 504 (1981).
(4) (a) A. Sharma and J. C. Joshi, *J. Quant. Spectrosc. Radiat. Transfer*, **12**, 1073 (1972); (b) The integrated intensity of the (4,0) band was chosen for normalizing the entire spectrum because it is the most intense and required the least amplification. Inspection of the records shows that all the bands drifted together. For example, after (4,0) decreased to 51%, (10,1) decreased to 57% and after (4,0) decreased to 85%, (9,1) decreased to 84%. In this respect (4,0) is not unique.

0022-3654/84/2088-5039$01.50/0